HHS Public Access

Author manuscript

*Mol Psychiatry*. Author manuscript; available in PMC 2017 February 22.

Published in final edited form as:

*Mol Psychiatry*. 2017 March ; 22(3): 458–465. doi:10.1038/mp.2016.99.

# HCN channel dendritic targeting requires bipartite interaction with TRIP8b and regulates antidepressant-like behavioral effects

**Ye Han**[1,*], **Robert J. Heuermann**[1,*], **Kyle A. Lyman**[1,*], **Daniel Fisher**[1], **Quratul-Ain Ismail**[1], and **Dane M. Chetkovich**[1]

[1]Davee Department of Neurology and Clinical Neurosciences, Northwestern University, Chicago, IL 60611 USA

## Abstract

Major Depressive Disorder is a prevalent psychiatric condition with limited therapeutic options beyond monoaminergic therapies. Although effective in some individuals, many patients fail to respond adequately to existing treatments and new pharmacologic targets are needed. HCN channels regulate excitability in neurons and blocking HCN channel function has been proposed as a novel antidepressant strategy. However, systemic blockade of HCN channels produces cardiac effects that limit this approach. Knockout (KO) of the brain-specific HCN channel auxiliary subunit TRIP8b also produces antidepressant-like behavioral effects and suggests that inhibiting TRIP8b function could produce antidepressant-like effects without affecting the heart. We examined the structural basis of TRIP8b-mediated HCN channel trafficking and its relationship to antidepressant-like behavior using a viral rescue approach in TRIP8b KO mice. We found that restoring TRIP8b to the hippocampus was sufficient to reverse the impaired HCN channel trafficking and antidepressant-like behavioral effects caused by TRIP8b KO. Moreover, we found that hippocampal expression of a mutated version of TRIP8b further impaired HCN channel trafficking and increased the antidepressant-like behavioral phenotype of TRIP8b KO mice. Thus, modulating the TRIP8b-HCN interaction bidirectionally influences channel trafficking and antidepressant-like behavior. Overall, our work suggests that small molecule inhibitors of the interaction between TRIP8b and HCN should produce antidepressant-like behaviors and could represent a new paradigm for the treatment of Major Depressive Disorder.

## Introduction

Major Depressive Disorder (MDD) is a common mental illness that causes tremendous health and social issues worldwide[1, 2]. Pharmacological treatment of MDD consists primarily of drugs targeting monoaminergic neurotransmitters, but there is a need for additional therapeutic options because many patients fail to respond to these therapies. Recent evidence suggests that changes in excitability within neural circuits of the



**Contact Information:** 303 E. Chicago Ave., Ward Building 10-201, Chicago, IL 60611, USA. d-chetkovich@northwestern.edu.
*These authors contributed equally to this work

**Conflict of Interests Statement**

The authors declare no conflicts of interest.

hippocampus may play an important role in MDD[3–5]. These findings raise the possibility that therapies affecting cellular excitability could function as novel antidepressants[6, 7].

Hyperpolarization-activated cyclic nucleotide-gated (HCN) channels are encoded by four pore-forming subunits (HCN1–4) and mediate $I_h$, a cationic current that regulates neuronal excitability[8, 9]. In pyramidal neurons of hippocampal area CA1, HCN channels are enriched in distal dendrites where they reduce network excitability by limiting integration of synaptic inputs and dampening $Ca^{2+}$ signaling[10–12]. This unique subcellular distribution of HCN channels is regulated by Tetratricopeptide repeat-containing Rab8b interacting protein (TRIP8b), an auxiliary subunit of HCN channels expressed uniquely in the nervous system[13–16]. Loss of TRIP8b eliminates the distal dendritic enrichment of HCN channels in pyramidal neurons of CA1 and leads to increased hippocampal excitability[16]. Knockdown of HCN1 in CA1[17] and genetic ablation of HCN1, HCN2, or TRIP8b[16] all produce an increase in neuronal excitability and, interestingly, all lead to antidepressant-like effects on behavior. Although these results suggest that blocking HCN channels could be useful in treating MDD, the important role of $I_h$ in cardiac function limits the clinical utility of systemic pharmacological blockade. Because TRIP8b is not expressed in the heart, we reasoned that disrupting the interaction between TRIP8b and HCN could increase hippocampal excitability and produce antidepressant-like behavioral effects without affecting HCN channels in the heart. In this paper, we establish the importance of the interaction between TRIP8b and HCN channels for channel trafficking and antidepressant-like behavioral effects.

TRIP8b binds to HCN pore-forming subunits at two distinct sites[18, 19]. While both sites independently influence subcellular trafficking in heterologous expression systems[18, 19], it is less clear how the distinct interactions affect channel function and behavior in the brain. To define the importance of the two TRIP8b-HCN interactions *in vivo*, we used adeno-associated viral (AAV) vectors to express wild type and mutant TRIP8b in the hippocampus of TRIP8b knockout (KO) mice. We found that restoring TRIP8b expression in CA1 neurons is sufficient to rescue the enrichment of HCN channels in CA1 pyramidal neuron distal dendrites and reverse the antidepressant-like behavior of TRIP8b KO mice. Mutating either interaction site prevented TRIP8b-mediated restoration of channel trafficking and reversal of antidepressant-like behavior. However, a mutant TRIP8b construct lacking the ability to interact with the HCN channel at its C-terminal tail further reduced the expression of HCN channels in dendrites of TRIP8b KO mice and increased their antidepressant-like behavior. These experiments demonstrate that disrupting either TRIP8b-HCN binding site interferes with HCN channel trafficking and function. Overall, our data suggest that disrupting the protein-protein interactions between TRIP8b and HCN channel pore-forming subunits should produce antidepressant-like behavioral effects and that targeting the interaction between TRIP8b and the HCN channel C-terminal tail may be particularly effective as a potential new therapeutic approach for MDD.

## Materials and Methods

### Mice

All animal experiments were performed according to protocols approved by the Institutional Animal Care and Use Committees of Northwestern University.

### Viral injections

Commercially generated AAV (Penn Vector) were prepared using custom plasmids and injected into the CA1 cell body layer of mice under stereotaxic control. AAV2/8 serotype was chosen to ensure high expression levels in the CA1 with minimal inflammation[20]. See Supplementary Information for details.

### Immunohistochemistry and Electrophysiology

Experiments were performed as described elsewhere, see Supplementary Information for details[21].

## Results

### Viral expression of TRIP8b rescues $I_h$ in CA1 pyramidal neurons of TRIP8b KO mice

TRIP8b KO mice lack all TRIP8b isoforms and have a reduction in both the distal dendritic enrichment of HCN channels and somatic $I_h$ in CA1 pyramidal neurons[16]. Although TRIP8b has many splice isoforms, previous work has shown that an isoform comprised of exons 1a, 4, and exons 5–16 (TRIP8b(1a-4)) is the most common[13, 22]. Thus we began by determining if this isoform is sufficient to rescue HCN channel distal dendritic enrichment. We generated an AAV carrying TRIP8b (Figure 1A, AAV-TRIP8b-IRES-eGFP, hereafter referred to as AAV-TRIP8b) driven by the human *synapsin* promoter in order to restrict expression to neurons (Supplementary Figure 1). To investigate if AAV-TRIP8b rescues somatic $I_h$, we bilaterally injected the CA1 of TRIP8b KO mice with AAV-eGFP or AAV-TRIP8b and injected wild type (WT) mice with AAV-eGFP as a positive control. We then made whole-cell recordings from the eGFP-labeled CA1 pyramidal neurons. As expected, AAV-eGFP did not influence $I_h$ in wild type or TRIP8b KO pyramidal neurons. In response to hyperpolarizing current injections, WT pyramidal neurons transduced with control AAV-eGFP displayed a voltage sag characteristic of $I_h$, which was noticeably reduced in TRIP8b KO mice transduced with AAV-eGFP. TRIP8b KO mice transduced with AAV-TRIP8b showed rescue of the sag ratio (Figure 1C/D, measured as $\Delta V_{max}/\Delta V_{steady\text{-}state}$). Voltage clamp measurements of $I_h$ produced similar results (Figure 1E/F). Expression of AAV-TRIP8b in TRIP8b KO mice yielded large, slowly activating inward currents in response to hyperpolarizing voltage steps that were significantly larger than currents recorded from AAV-eGFP control neurons. Although robust $I_h$ changes were detected in our recordings, no change in either resting membrane potential or input resistance was noted (Table S1). One potential explanation for these findings is that resting membrane potential and input resistance are not uniquely dependent on $I_h$ and compensatory changes in other currents might attenuate changes in these properties. It is also possible that cell-to-cell variability in AAV-mediated TRIP8b expression masked changes in these parameters.

After determining that AAV-TRIP8b was sufficient to rescue somatic $I_h$, we next investigated its effect on distal dendritic enrichment by unilaterally injecting the viral constructs in TRIP8b KO mice and performing immunohistochemistry (IHC). In the uninjected hemisphere of all conditions, the distal dendritic enrichment of HCN1 and HCN2 was markedly reduced, similar to our previous findings[16]. In TRIP8b KO mice injected with AAV-eGFP, no distal dendritic enrichment of HCN1 or HCN2 was noted in the injected hemisphere (Supplementary Figure S2). In contrast, unilateral injection of AAV-TRIP8b led to successful rescue of the distal dendritic enrichment of HCN1 and HCN2 (Figure 2A). To quantify this effect, we scaled the magnitude of HCN1 staining in the injected hemisphere by the staining in the uninjected hemisphere using regions of interest (ROI) drawn over each anatomic structure (Figure 2B). As expected, AAV-TRIP8b produced an increase in HCN1 staining in the distal dendrites of the stratum lacunosum-moleculare (SLM; Figure 2B) and in HCN protein on western blot (Supplementary Figure S3). These experiments demonstrate that viral rescue of TRIP8b in the hippocampus is sufficient to rescue HCN channel trafficking.

## CA1 presynaptic inhibitory terminals express HCN1 in a TRIP8b-independent manner

Incidentally, we noted that HCN1 expression in the cell body layer of CA1 appeared punctate, suggesting that it was expressed by terminals synapsing onto the cell bodies of CA1 pyramidal neurons. We subsequently performed immunohistochemistry to confirm that indeed, the majority of HCN1 in the cell body layer is colocalized with vesicular GABA transporter (vGAT)-positive inhibitory terminals (Supplementary Figure S4). Similar experiments using a presynaptic excitatory marker (vGlut) and postsynaptic markers (PSD95, Gephrin) did not show colocalization (data not shown). As has been seen at other presynaptic terminals expressing HCN1[23], punctate HCN1 expression in the CA1 cell body layer was not changed in TRIP8b KO mice, suggesting that TRIP8b is not responsible for trafficking HCN1 to axonal terminals in these interneurons. Given that we used a *synapsin* promoter in our AAV, it remained possible that exogenous expression of TRIP8b in the interneurons affected HCN1 trafficking. However, we did not observe any change in the presynaptic localization of HCN1 after treatment with either AAV-eGFP or AAV-TRIP8b (Supplementary Figure S5). Given that HCN1 expression in CA1 interneurons did not change with genetic knockout of TRIP8b or viral expression of TRIP8b, we did not pursue these findings further.

## Loss of the distal dendritic enrichment of HCN channels in CA1 is responsible for the increase in antidepressant-like behavior of TRIP8b KO mice

Previous reports have found that reduction of HCN channel expression by HCN1 or HCN2 knockout[16] leads to antidepressant-like effects on behavior in two common antidepressant screening tests: the Forced Swim Test (FST) and Tail Suspension Test (TST). Because genetic ablation of TRIP8b[16] and siRNA knockdown of HCN1 in CA1 pyramidal neurons[17] also lead to antidepressant-like effects on behavior, we reasoned there could be a specific link between antidepressant-like behavioral effects and the distal dendritic enrichment of HCN channels in CA1 dendrites. We next examined if rescuing the distal dendritic enrichment of HCN channels influenced performance on TST and FST. We injected the CA1 of TRIP8b KO mice bilaterally with either an AAV-eGFP control or AAV-TRIP8b, which

restored HCN channel distal dendritic enrichment in CA1 pyramidal neurons. We then performed FST and TST (Figure 2 C/D). As demonstrated previously, TRIP8b KO mice have reduced immobility time on both FST and TST compared to WT littermates. TRIP8b KO mice injected with AAV-TRIP8b showed increased immobility time on TST and FST compared to AAV-eGFP injected controls, indicating a reversal of the antidepressant-like behavior normally observed in TRIP8b KO mice. As a control for locomotor function, we also performed an open field test (Supplementary Figure S4). Consistent with a specific effect on TST and FST, no differences were observed between AAV-eGFP and AAV-TRIP8b treated mice. Our results indicate that rescuing the distal dendritic enrichment of HCN channels with bilateral AAV-TRIP8b injection is sufficient to reverse the behavioral phenotype of TRIP8b KO mice.

## Both TRIP8b binding sites are required for distal dendritic enrichment of HCN channels

We next set out to identify the TRIP8b domains that are necessary for HCN channel trafficking. All TRIP8b isoforms bind to HCN subunits at two distinct locations. First, there is an interaction between the cyclic nucleotide binding domain (CNBD) of HCN channels and an acidic stretch of amino acids N-terminal to the tetratricopeptide repeat (TPR) domains of TRIP8b[15, 24]. Second, the TPR domains of TRIP8b bind to the C-terminal tail of HCN. To examine the role of each interaction site *in vivo* we generated AAVs to express TRIP8b mutants designed to selectively eliminate each binding site. We previously demonstrated that deletion of 58 amino acids in the N-terminal portion of TRIP8b common to all isoforms (TRIP8b(Δ58)) disrupts interaction with the CNBD of HCN subunits without blocking the interaction between TRIP8b and the HCN subunit C-terminal tail[19]. Conversely, mutation of a key asparagine residue in the C-terminal portion of TRIP8b – the 13$^{th}$ residue of the third TPR domain (N13A) – disrupts binding to HCN subunit C-terminal tails while leaving the CNBD interaction intact[19]. To determine the importance of each TRIP8b-HCN interaction site for HCN channel surface trafficking *in vivo*, we performed whole cell recordings from TRIP8b KO mice bilaterally injected with AAV-eGFP, AAV-TRIP8b(N13A) (Figure 3Ai, hereafter referred to be as AAV-N13A), or AAV-TRIP8b(Δ58) (Figure 3Aii, hereafter referred to be as AAV-Δ58). Interestingly, mutation of either binding site prevented the TRIP8b constructs from successfully rescuing the sag ratio (Figure 3B/D) or $I_h$ amplitude (Figure 3C/E), indicating that both sites are necessary for TRIP8b-mediated upregulation of $I_h$ *in vivo*.

Although mutation of either TRIP8b binding site prevented restoration of $I_h$ in our whole cell recordings, somatic recordings of CA1 pyramidal neurons may not detect small changes in ion channel function in the distal dendrites[22]. This is especially problematic in the TRIP8b KO animals that express substantially fewer HCN channels than wild type animals[16]. We therefore unilaterally injected TRIP8b KO mice with one of the viral constructs mentioned above (AAV-eGFP, AAV-N13A, AAV-Δ58), or AAV-TRIP8b(Δ58/N13A), a double mutant lacking the ability to bind HCN subunits at either binding site (Figure 3Aiii, hereafter referred to be as an AAV-Δ58/N13A). We then performed IHC and quantified our images as above. We found that none of the mutants could restore HCN subunit distal dendritic enrichment (Figure 4 for HCN1, see Supplementary Figure S6 for

HCN2). These results indicate that both TRIP8b-HCN interaction sites are necessary for enriching HCN channels in distal CA1 dendrites.

Surprisingly, AAV-N13A decreased dendritic HCN1 signal intensity relative to AAV-eGFP injected TRIP8b KO mice, suggesting that the isolated loss of the interaction between TRIP8b and the HCN C-terminal tail may actively restrict dendritic targeting of HCN channels. We subsequently performed western blots from hippocampi of TRIP8b KO mice bilaterally injected with each TRIP8b mutant and noted a reduction in HCN1 and HCN2 total protein after injection with AAV-N13A relative to other conditions (Supplementary Figure S7), confirming a 'gain-of-function' effect of the AAV-N13A mutant to actively reduce total HCN protein levels.

Since the mutant TRIP8b constructs failed to rescue distal dendritic enrichment, we reasoned they should not reverse the antidepressant-like behavior of TRIP8b KO mice. We bilaterally injected TRIP8b KO mice with AAV-N13A, AAV-Δ58, or AAV-eGFP as a control. Consistent with our electrophysiological and IHC results, bilateral injection of AAV-Δ58 did not produce a change in either TST or FST (Figure 4). Remarkably, expression of AAV-N13A, which diminished dendritic HCN channel expression without affecting somatic $I_h$, reduced the immobility time during FST and TST even more than in KO animals injected with AAV-eGFP. To ensure that these differences in FST and TST were not the result of increased locomotor activity, we performed an open field test (Supplementary Figure S8) and detected no differences in locomotion between groups. These results demonstrate that the interaction between TRIP8b and both the CNBD and C-terminal tail binding sites is required to maintain proper distal dendritic enrichment of HCN channels *in vivo*. In addition, both interaction sites are also necessary for reversing the antidepressant-like behavior of TRIP8b KO mice. Finally, the surprising finding that the N13A mutation, which prohibits TRIP8b interaction with the HCN subunit C-terminal tail, actively inhibits the distal dendritic enrichment of HCN channels hints at a novel regulatory mechanism of HCN channel trafficking. These results show that manipulations of TRIP8b-HCN coupling lead to changes in the distal dendritic enrichment of the channels and that this distal dendritic trafficking is inversely correlated with antidepressant-like behavior.

## Discussion

Genetic knockout of HCN1 or HCN2[16], as well as siRNA knockdown of HCN1 in the CA1[17], leads to antidepressant-like effects on behavior in the TST and FST. Importantly, the antidepressant-like behavior of the HCN1 and HCN2 KO mice is also observed in TRIP8b KO mice[16]. Because a critical role for TRIP8b in the CA1 is to facilitate the proper subcellular trafficking of HCN channels, these results suggest that the distal dendritic enrichment of HCN channels produced by TRIP8b is particularly relevant for influencing antidepressant-like behaviors. In this paper, we demonstrate that bidirectionally manipulating the distal dendritic enrichment of HCN channels in CA1 is sufficient to influence antidepressant-like behaviors. Bilateral injection of AAV-TRIP8b restored the distal dendritic enrichment of HCN channels and reversed the antidepressant-like behaviors of TRIP8b knockout, while bilateral injection of AAV-N13A reduced the distal dendritic enrichment of HCN channels and promoted antidepressant-like behaviors.

Other studies have also pointed to a role for HCN channels in depression. Mice subjected to Chronic Social Defeat (CSD) stress develop depression-like behaviors, and a recent report demonstrated that $I_h$ is significantly upregulated in NAc-projecting, VTA dopaminergic neurons[25]. Interestingly, chronic SSRI administration reduced the increase in $I_h$ caused by CSD stress[26]. Corticotropin releasing factor, which has been implicated in depression pathogenesis through HPA axis dysfunction[27], increases $I_h$ in both the basolateral amygdala and paraventricular nucleus of the hypothalamus[28, 29]. While evidence is accumulating for involvement of HCN channels in depression models, it remains to be determined if upregulation of HCN channels in distinct brain regions underlies depression. Future studies should also indicate whether upregulation of HCN or TRIP8b in hippocampal area CA1 occurs in MDD patients or rodent models and whether reducing HCN channel function in the hippocampus underlies any of the clinical effects of monoamine reuptake inhibitors.

The precise mechanism for how removal of dendritic HCN channels produces antidepressant-like behavior remains unclear. An accumulating body of evidence suggests that MDD is caused by dysfunction in many identifiable neuronal circuits. One recent report showed that chronic stress decreased both CA1 and hippocampal network excitability and that this decrease was reversible with antidepressants[30]. Loss of HCN channels from hippocampal distal dendrites increases temporal summation and cellular excitability, and in the context of the neuronal circuit hypothesis, increasing hippocampal network excitability is a plausible mechanism by which loss of HCN channels could influence antidepressant-like behavior. In addition, the specific localization of HCN channels to the distal dendrites of CA1, which receive selective input from the entorhinal cortex, may confer a pathway-specific regulation of excitability. Chronic stress in mice decreases EPSPs in the SLM of CA1 pyramidal cells through AMPA-R downregulation[31]. In addition, chronic SSRI treatment specifically reverses these AMPA-R mediated decreases in excitability of SLM synapses without changing the excitability of more proximal synapses[32]. Because HCN channels are enriched in the SLM, where they constrain excitability of temporoammonic inputs, loss of HCN channels in these distal dendrites could reverse or mitigate pathway-specific synaptic weakening that may play a role in depression-like behaviors.

In this paper, we establish the distal dendritic enrichment of HCN channels in CA1 pyramidal neurons as a key determinant of performance in the tail suspension test and forced swim test. For therapeutic purposes, it is significant to note that therapies aimed at disrupting either TRIP8b-HCN interaction site are predicted to limit trafficking of HCN channels and produce an increase in antidepressant-like behavior. Recent efforts have been directed at finding small molecule inhibitors of the interaction between the TPR domains of TRIP8b and the C-terminal tripeptide of HCN channel pore-forming subunits[33]. Given the brain-specific expression pattern of TRIP8b, this strategy should limit cardiac effects seen with systemic HCN channel inhibitors. Overall, our results indicate that disrupting the distal dendritic enrichment of HCN channels through manipulations that impair TRIP8b-HCN interactions represents a promising target for future antidepressant therapies[33].

## Supplementary Material

Refer to Web version on PubMed Central for supplementary material.

## Acknowledgments

This work was supported by National Institutes of Health Grant 2R01NS059934, R01MH106511 and R21MH104471 (D.M.C), Brain Research Foundation SG 2012-01 (D.M.C.), Chicago Biomedical Consortium HTS-004 (Y.H. and D.M.C) and National Institutes of Health Grant 2T32MH067564 (K.A.L).

## References

1. Kessler RC, Berglund P, Demler O, Jin R, Merikangas KR, Walters EE. Lifetime prevalence and age-of-onset distributions of DSM-IV disorders in the National Comorbidity Survey Replication. Arch Gen Psychiatry. 2005; 62:593–602. [PubMed: 15939837]
2. Lépine J-P, Briley M. The increasing burden of depression. Neuropsychiatr Dis Treat. 2011; 7:3–7. [PubMed: 21750622]
3. Krishnan V, Nestler EJ. The molecular neurobiology of depression. Nature. 2008; 455:894–902. [PubMed: 18923511]
4. Duman RS, Aghajanian GK. Synaptic Dysfunction in Depression: Potential Therapeutic Targets. Science. 2012; 338:68–72. [PubMed: 23042884]
5. Russo SJ, Nestler EJ. The brain reward circuitry in mood disorders. Nat Rev Neurosci. 2013; 14:609–625. [PubMed: 23942470]
6. Newport DJ, Carpenter LL. Ketamine and other NMDA antagonists: early clinical trials and possible mechanisms in depression. Am J Psychiatry. 2015; 172:950–966. [PubMed: 26423481]
7. Papakostas GI, Ionescu DF. Towards new mechanisms: an update on therapeutics for treatment-resistant major depressive disorder. Mol Psychiatry. 2015; 20:1142–1150. [PubMed: 26148812]
8. Biel M, Wahl-Schott C, Michalakis S, Zong X. Hyperpolarization-activated cation channels: from genes to function. Physio Rev. 2009; 89:847–885.
9. Wahl-Schott C, Biel M. HCN channels: structure, cellular regulation and physiological function. Cell Mol Life Sci. 2009; 66:470–494. [PubMed: 18953682]
10. Magee JC. Dendritic hyperpolarization-activated currents modify the integrative properties of hippocampal CA1 pyramidal neurons. J Neurosci. 1998; 18:7613–7624. [PubMed: 9742133]
11. Magee J. Dendritic Ih normalizes temporal summation in hippocampal CA1 neurons. Nat Neurosci. 1999; 2:848–848.
12. Tsay D, Dudman JT, Siegelbaum SA. HCN1 channels constrain synaptically evoked Ca2+ spikes in distal dendrites of CA1 pyramidal neurons. Neuron. 2007; 56:1076–1089. [PubMed: 18093528]
13. Santoro B, Piskorowski RA, Pian P, Hu L, Liu H, Siegelbaum SA. TRIP8b splice variants form a family of auxiliary subunits that regulate gating and trafficking of HCN channels in the brain. Neuron. 2009; 62:802–813. [PubMed: 19555649]
14. Zolles G, Wenzel D, Bildl W, Schulte U, Hofmann A, Muller CS, et al. Association with the auxiliary subunit PEX5R/Trip8b controls responsiveness of HCN channels to cAMP and adrenergic stimulation. Neuron. 2009; 62:814–815. [PubMed: 19555650]
15. Lewis AS, Schwartz E, Chan CS, Noam Y, Shin M, Wadman WJ, et al. Alternatively spliced isoforms of TRIP8b differentially control h channel trafficking and function. J Neurosci. 2009; 29:6250–6265. [PubMed: 19439603]
16. Lewis AS, Vaidya SP, Blaiss CA, Liu Z, Stoub TR, Brager DH, et al. Deletion of the hyperpolarization-activated cyclic nucleotide-gated channel auxiliary subunit TRIP8b impairs hippocampal Ih localization and function and promotes antidepressant behavior in mice. J Neurosci. 2011; 31:7424–7440. [PubMed: 21593326]
17. Kim CS, Chang PY, Johnston D. Enhancement of dorsal hippocampal activity by knockdown of HCN1 channels leads to anxiolytic- and antidepressant-like behaviors. Neuron. 2012; 75:503–516. [PubMed: 22884333]
18. Santoro B, Hu L, Liu H, Saponaro A, Pian P, Piskorowski RA, et al. TRIP8b regulates HCN1 channel trafficking and gating through two distinct C-terminal interaction sites. J Neurosci. 2011; 31:4074–4086. [PubMed: 21411649]
19. Han Y, Noam Y, Lewis AS, Gallagher JJ, Wadman WJ, Baram TZ, et al. Trafficking and gating of hyperpolarization-activated cyclic nucleotide-gated channels are regulated by interaction with

tetratricopeptide repeat-containing Rab8b-interacting protein (TRIP8b) and cyclic AMP at distinct sites. J Biol Chem. 2011; 286:20823–20834. [PubMed: 21504900]

20. Aschauer DF, Kreuz S, Rumpel S. Analysis of Transduction Efficiency, Tropism and Axonal Transport of AAV Serotypes 1, 2, 5, 6, 8 and 9 in the Mouse Brain. PLoS ONE. 2013; 8:e76310. [PubMed: 24086725]
21. Heuermann RJ, Jaramillo TC, Ying S-W, Suter BA, Lyman KA, Han Y, et al. Reduction of thalamic and cortical Ih by deletion of TRIP8b produces a mouse model of human absence epilepsy. Neurobiol Dis. 2016; 85:81–92. [PubMed: 26459112]
22. Piskorowski R, Santoro B, Siegelbaum SA. TRIP8b splice forms act in concert to regulate the localization and expression of HCN1 channels in CA1 pyramidal neurons. Neuron. 2011; 70:495–509. [PubMed: 21555075]
23. Huang Z, Lujan R, Martinez-Hernandez J, Lewis AS, Chetkovich DM, Shah MM. TRIP8b-independent trafficking and plasticity of adult cortical presynaptic HCN1 channels. J Neurosci. 2012; 32:14835–14848. [PubMed: 23077068]
24. Saponaro A, Pauleta SR, Cantini F, Matzapetakis M, Hammann C, Donadoni C, et al. Structural basis for the mutual antagonism of cAMP and TRIP8b in regulating HCN channel function. Proc Natl Sci U S A. 2014; 111:14577–14582.
25. Friedman AK, Walsh JJ, Juarez B, Ku SM, Chaudhury D, Wang J, et al. Enhancing depression mechanisms in midbrain dopamine neurons achieves homeostatic resilience. Science. 2014; 344:313–319. [PubMed: 24744379]
26. Cao JL, Covington HE, Friedman AK, Wilkinson MB, Walsh JJ, Cooper DC, et al. Mesolimbic Dopamine Neurons in the Brain Reward Circuit Mediate Susceptibility to Social Defeat and Antidepressant Action. J Neurosci. 2010; 30:16453–16458. [PubMed: 21147984]
27. Joëls M, Baram TZ. The neuro-symphony of stress. Nat Rev Neurosci. 2009; 10:459–466. [PubMed: 19339973]
28. Qiu DL, Chu CP, Shirasaka T, Tsukino H, Nakao H, Kato K, et al. Corticotrophin-releasing factor augments the IH in rat hypothalamic paraventricular nucleus parvocellular neurons in vitro. J Neurophysiol. 2005; 94:226–234. [PubMed: 15800070]
29. Giesbrecht CJ, Mackay JP, Silveira HB, Urban JH, Colmers WF. Countervailing Modulation of Ih by Neuropeptide Y and Corticotrophin-Releasing Factor in Basolateral Amygdala As a Possible Mechanism for Their Effects on Stress-Related Behaviors. J Neurosci. 2010; 30:16970–16982. [PubMed: 21159967]
30. Stepan J, Hladky F, Uribe A, Holsboer F, Schmidt MV, Eder M. High-Speed imaging reveals opposing effects of chronic stress and antidepressants on neuronal activity propagation through the hippocampal trisynaptic circuit. Front Neural Circuits. 2015; 9:819.
31. Kallarackal AJ, Kvarta MD, Cammarata E, Jaberi L, Cai X, Bailey AM, et al. Chronic Stress Induces a Selective Decrease in AMPA Receptor-Mediated Synaptic Excitation at Hippocampal Temporoammonic-CA1 Synapses. J Neurosci. 2013; 33:15669–15674. [PubMed: 24089474]
32. Cai X, Kallarackal AJ, Kvarta MD, Goluskin S, Gaylor K, Bailey AM, et al. Local potentiation of excitatory synapses by serotonin and its alteration in rodent models of depression. Nat Neurosci. 2013; 16:464–472. [PubMed: 23502536]
33. Han Y, Lyman K, Clutter M, Schiltz GE. Identification of Small-Molecule Inhibitors of Hyperpolarization-Activated Cyclic Nucleotide–Gated Channels. J Biomol Screen. 2015; 20:1124–1131. [PubMed: 26045196]
34. Lein ES, Hawrylycz MJ, Ao N, Ayres M, Bensinger A, Bernard A, et al. Genome-wide atlas of gene expression in the adult mouse brain. Nature. 2007; 445:168–176. [PubMed: 17151600]

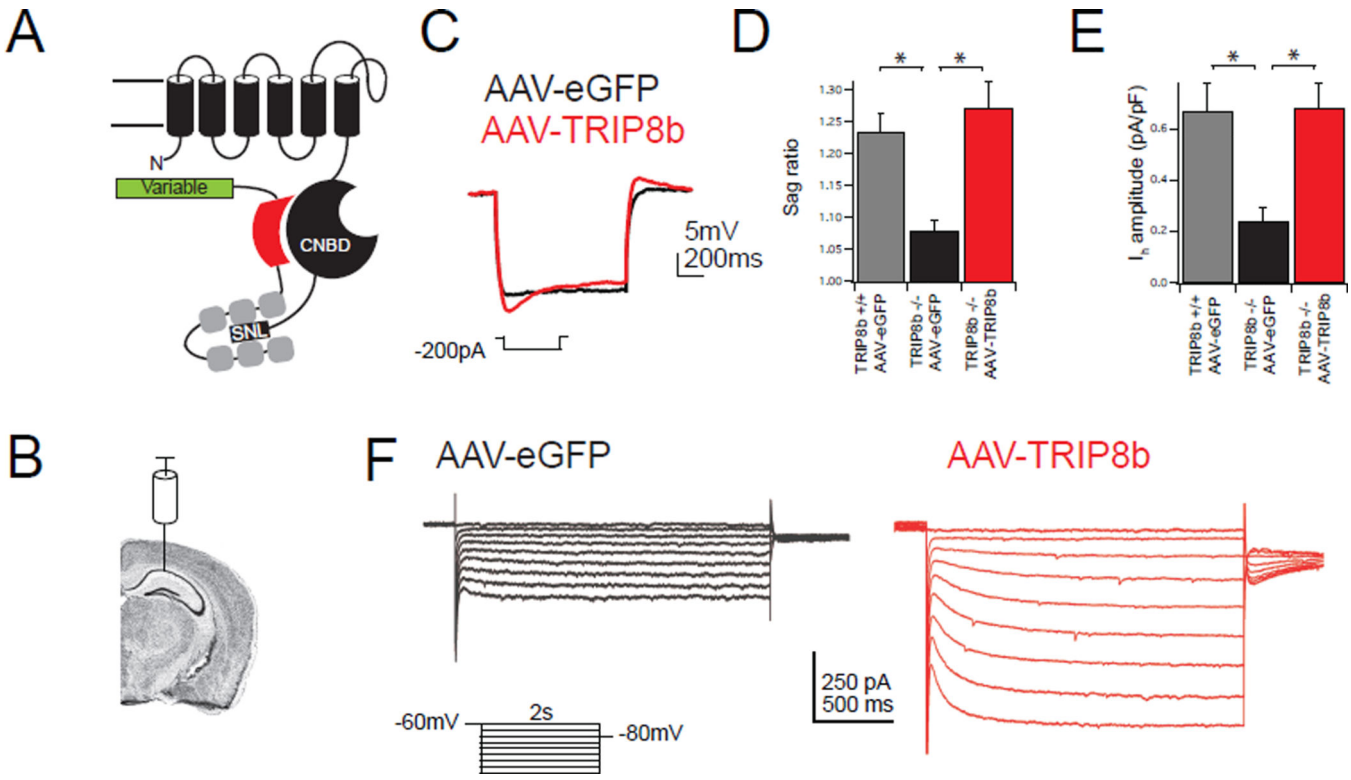


**Figure 1. Viral expression of TRIP8b is sufficient to rescue $I_h$**

**A.**) Schematic of TRIP8b interacting with a single HCN pore-forming subunit. The N-terminal interaction occurs between the CNBD of HCN and an acidic stretch of amino acids in TRIP8b, schematized by a red shape. The C-terminal tail interaction occurs between the TPR domains of TRIP8b in gray and the 'SNL' tripeptide of HCN1, 2, and 4. The variably spliced N terminus of TRIP8b is represented by a green rectangle. **B.)** Schematic showing virus injection site. Coronal brain image generated using the Allen Mouse Brain Atlas[34]. **C.)** Whole-cell somatic recordings from eGFP-positive CA1 pyramidal neurons four weeks after bilateral viral injection into TRIP8b KO mice. Representative traces are shown during hyperpolarizing current injection. **D.)** Quantification of sag ratio. For reference, WT mice injected with AAV-eGFP are also shown (WT: 1.23±0.02, n=8; AAV-eGFP: 1.07±0.01, n=9; AAV-TRIP8b: 1.27±0.04, n=8; $(F(2,22)=11.64, p<0.001)$. **E.)** Quantification of $I_h$ amplitude from somatic voltage-clamp recordings from TRIP8b KO animals injected with the indicated viral construct (AAV-eGFP: 0.24±0.05pA/pF, n=9, AAV-TRIP8b: 0.68±0.10pA/pF, n=7). AAV-eGFP injected wild type mice are included for reference (0.67±0.11 pA, n=8; $F(2,21)=7.92, p<0.01$). **F.)** Representative voltage-clamp traces in response to hyperpolarizing voltage steps. All error bars represent ± s.e.m and are described above as mean ± s.e.m. *$p<0.05$ on Tukey's test following one way ANOVA.

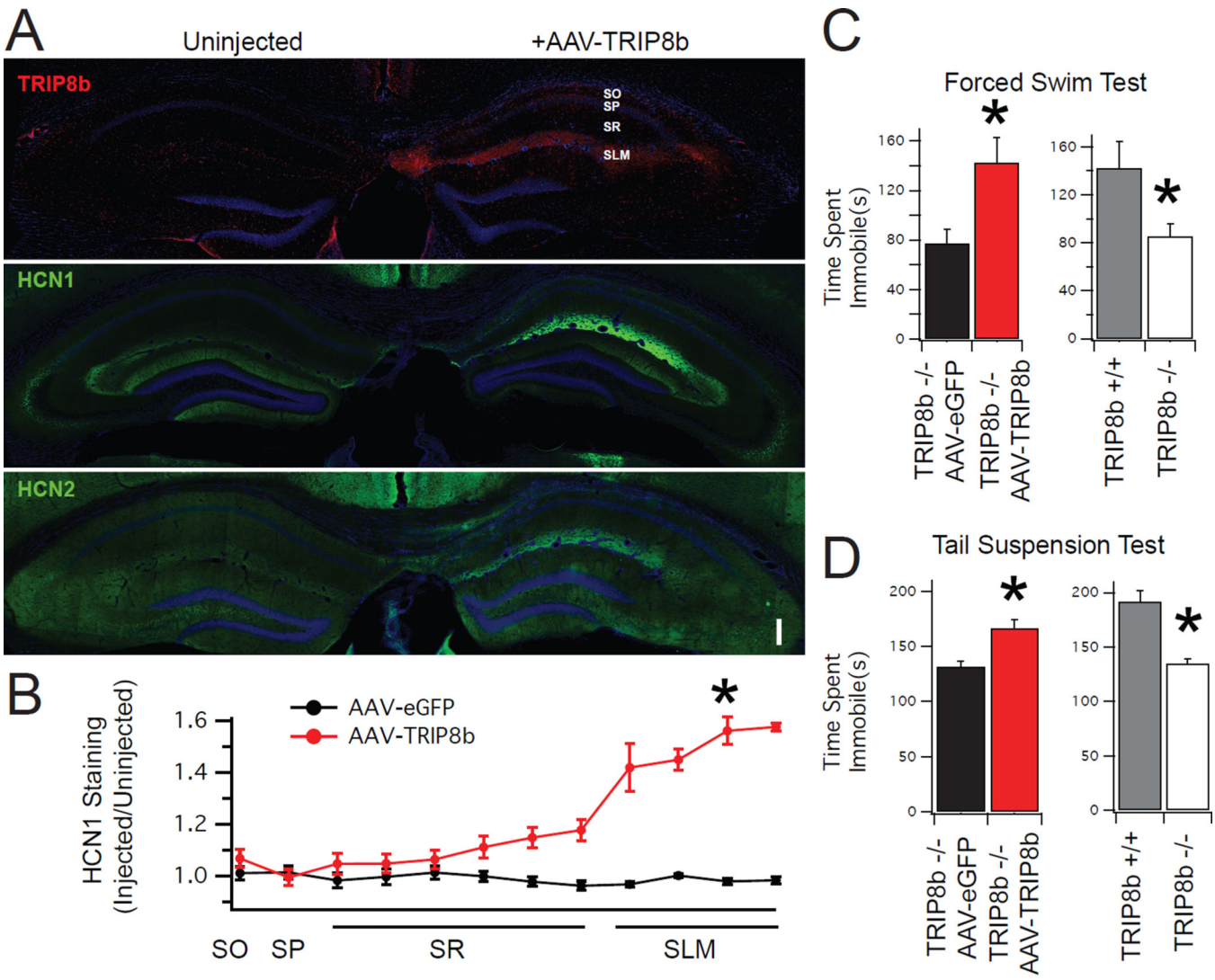


**Figure 2. Dendritic targeting of HCN channels is rescued by viral delivery of TRIP8b**

**A.)** Low power composite image of TRIP8b KO animals unilaterally injected with AAV-TRIP8b. Uninjected hemisphere (left) shows absence of TRIP8b (red, top panel) and weak hippocampal HCN gradients (green, middle and lower panels). Injected hemisphere (right) shows restoration of the distal dendritic enrichment of TRIP8b, HCN1, and HCN2. SO: Stratum oriens, SP: Stratum pyramidale, SR: Stratum radiatum, SLM: Stratum lacunosum moleculare. Scale bar represents 200 μm. **B.)** Quantification of HCN1 channel expression after viral rescue. A value of '1' represents no change in staining of HCN1 relative to the uninjected hemisphere. Asterisk denotes comparison of HCN1 staining in the SLM (AAV-eGFP: 0.98±0.01 n=6, AAV-TRIP8b= 1.52±0.05 n=4, t=23.81, p<0.001). **C/D)** TRIP8b KO mice bilaterally injected with AAV-TRIP8b showed more immobility time on forced swim test (FST) and tail suspension test (TST) relative to AAV-eGFP injected controls. Injection of AAV-TRIP8b increased the immobility time on TST (AAV-eGFP = 132±20.9 sec, AAV-TRIP8b 166.16±26.5 sec, t=2.47, p<0.05) and FST (AAV-eGFP = 77.3±11.2 sec, AAV-TRIP8b = 142.8±20.1 sec, t=6.96, p<0.05), indicating a reversal of the increase in

antidepressant-like behavioral effects of TRIP8b KO mice (n=6,6). For comparison, uninjected wild type mice and uninjected TRIP8b KO mice are also shown to highlight the increase in antidepressant-like behavior for both TST (WT = 191.8±17.6 sec, TRIP8b KO=134.8±23.4 sec, $t=4.47$, $p<0.05$) and FST (WT=142.4±21.8 sec, TRIP8b KO=85.6±9.93 sec, $t=5.72$, $p<0.05$) (n=6,5). Note that the comparison between AAV-eGFP and AAV-TRIP8b is distinct from the comparison between wild type and TRIP8b KO mice because the AAV-eGFP/AAV-TRIP8b were both subject to bilateral viral injections while the other groups were not. *$P<0.05$ two tail unpaired T test. All error bars represent ± s.e.m. and are described above as mean ± s.e.m.

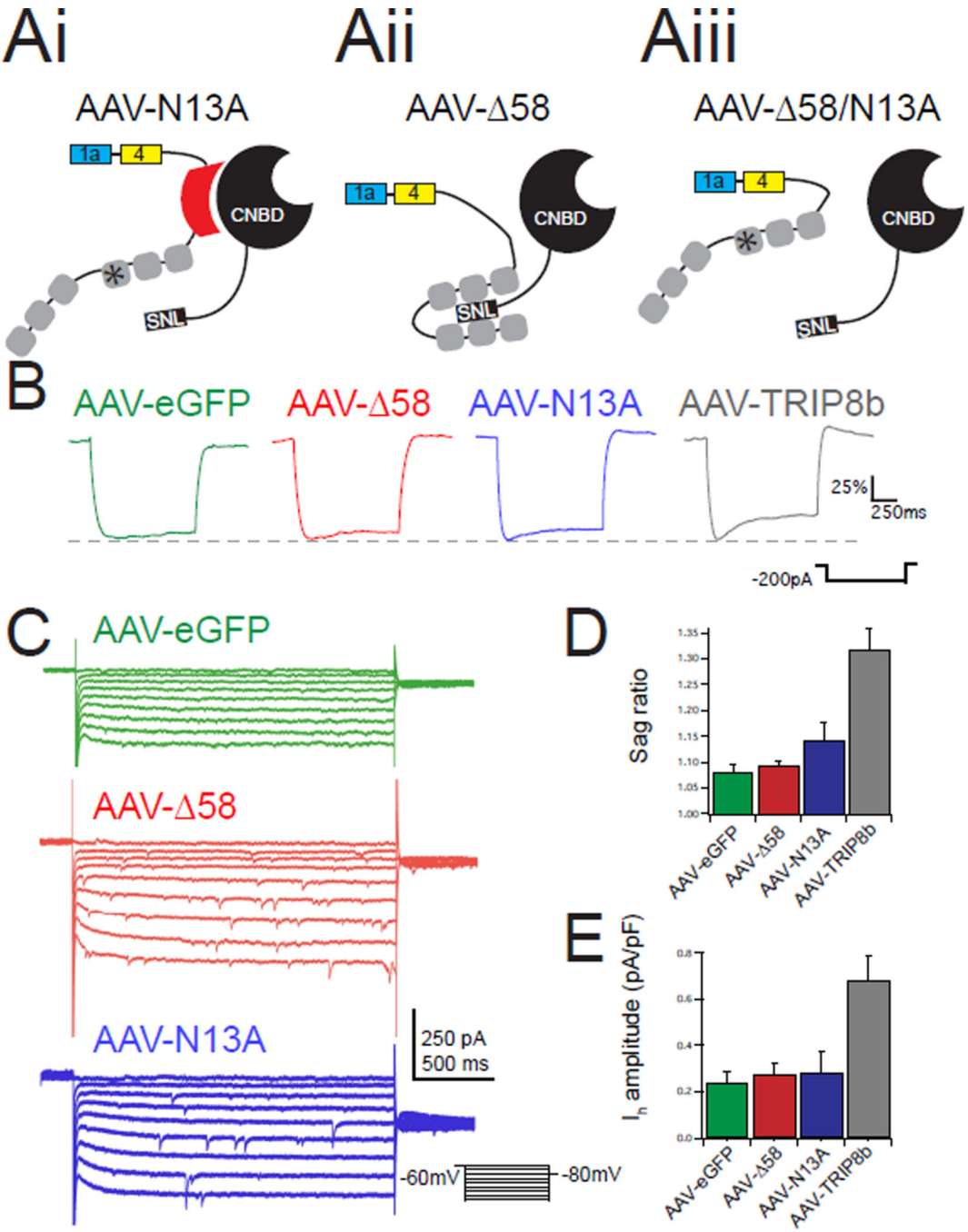


**Figure 3. Loss of either TRIP8b-HCN binding site blocks viral rescue of $I_h$**

**Ai–iii.)** Schematic of mutant TRIP8b isoforms used showing predicted results of mutating either binding site. **B.)** Representative traces from EGFP-positive CA1 pyramidal neurons from each condition during hyperpolarizing current injections. Traces are scaled to $\Delta V_{max}$ to facilitate comparison of sag ratio. **C.)** Representative voltage-clamp recordings in response to hyperpolarizing voltage steps highlight slowly activating inward current. **D.)** Quantification of the sag ratio showed no difference by ANOVA (AAV-eGFP: 1.07±0.01, n=9; AAV-N13A: 1.11±0.02, n=7; AAV-Δ58: 1.09±0.01, n=6; $F(2,19)=2.095$, $p>0.05$). For

comparison the sag ratio for AAV-TRIP8b infected neurons is reproduced from Figure 1. **E.)** Voltage-clamp measurements of $I_h$ also showed no difference by ANOVA). (AAV-eGFP: 0.24±0.05 pA/pF, n=9; AAV-N13A: 0.282±0.09 pA/pF, n=7; AAV-Δ58: 0.27±0.04 pA/pF, n=5; $F(2,19)=0.09$, $p>0.05$). For comparison, the $I_h$ amplitude from AAV-TRIP8b infected neurons is reproduced from Figure 1. All error bars represent ± standard error of the mean and are described above as mean ± s.e.m.

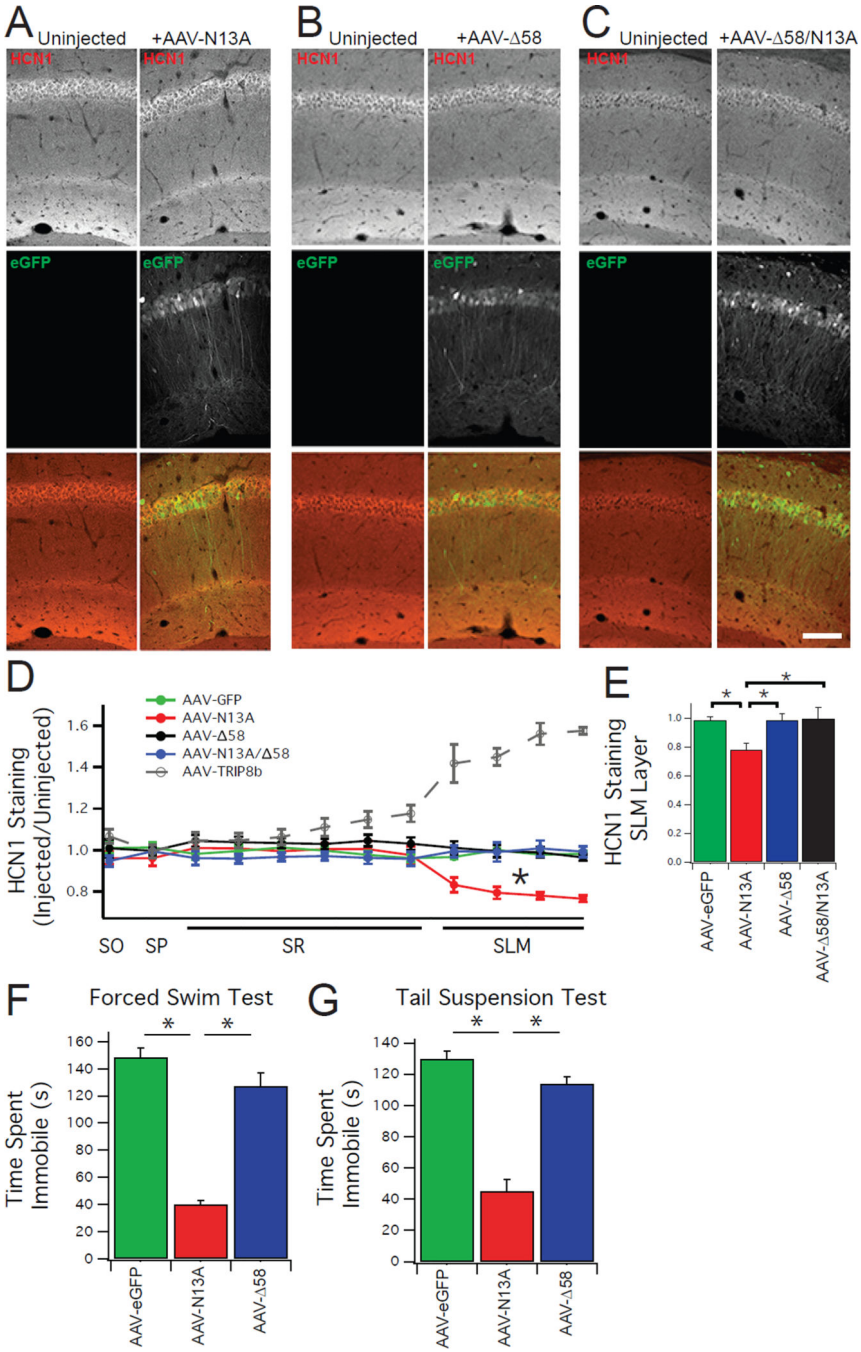


**Figure 4. Both TRIP8b-HCN binding sites are required for dendritic targeting of HCN channels**

**A.)** Confocal images demonstrating that unilateral injection of AAV-N13A causes a reduction in HCN1 staining in the SLM. Top panels show staining for HCN1 (red), middle panel shows staining for eGFP (green), and the bottom panel shows a composite image. Images in the left column are from the uninjected (control) hemisphere, while the right column shows the AAV-N13A injected hemisphere. **B/C.)** Unilateral injection of either AAV-Δ58 or AAV-Δ58/N13A fails to rescue HCN1 distal dendritic enrichment. Display of images is identical to that in **A.** Scale bar represents 100 μm. **D.)** Quantification of HCN1

distal enrichment. HCN1 staining intensity in regions of interest from the virally injected hemisphere were scaled by staining in the contralateral (uninjected) hemisphere. For comparison, the AAV-TRIP8b rescue experiment is reproduced from Figure 2. **E.)** Quantification of HCN1 staining in the SLM layer of CA1 (AAV-eGFP= 0.98±0.01, AAV-Δ58=0.98±0.04, AAV-N13A=0.78±0.04, AAV-Δ58/N13A=0.99±0.07). A one way ANOVA comparing staining intensity in the SLM of the different conditions (AAV-eGFP, AAV-Δ58, AAV-N13A, AAV-Δ58/N13A) was found to be significant ($F(3,17)=22.375$, $p<0.05$). Tukey's *post hoc* tests found a difference between AAV-N13A and AAV-eGFP ($p<0.05$), AAV-N13A and AAV-Δ58 ($p<0.05$), and AAV-N13A and AAV-N13A/Δ58 ($p<0.05$). A one way ANOVA comparing HCN1 staining in the cell body layer of the different conditions (AAV-eGFP, AAV-N13A, AAV-Δ58, AAV-Δ58/N13A) was not significant ($F(3,17)=0.59$, $p>0.5$) hence *post hoc* tests were not performed. **F.)** TRIP8b KO mice bilaterally injected with AAV-N13A, but not AAV-Δ58, show less immobility time on TST and FST. A one way ANOVA examining the immobility time on FST found a significant difference (AAV-eGFP=148.42±18.8 sec, AAV-N13A=40.2±6.7 sec, AAV-Δ58=127.4±25.0 sec, $F(2,18)=67.34$, $P<0.05$), and follow up Tukey's tests revealed a difference between AAV-eGFP and AAV-N13A as well as a difference between AAV-N13A and AAV-Δ58. **G.)** A one way ANOVA examining the immobility time on TST was significantly different (AAV-eGFP=130±12.2 sec, AAV-N13A=44.9±20.1 sec, AAV-Δ58=114±10.0 sec, $F(2,17)=62.32$, $p<0.05$) with Tukey's test showing differences between AAV-eGFP and AAV-N13A and between AAV-Δ58 and AAV-N13A. *$p<0.05$ on Tukey's HSD test following one way ANOVA. All error bars represent ± standard error of the mean and are described above as mean ± s.e.m.